Characterization, Machinability Studies and Multi-response Optimization of AA 6082 Hybrid Metal Matrix Composite

Ndudim Henry Ononiwu (219122653@student.uj.ac.za)
University of Johannesburg Faculty of Engineering and Built Environment https://orcid.org/0000-0001-7655-5932

Chigbogu G. Ozoegwu
University of Johannesburg South Africa

Nkosinathi Madushele
University of Johannesburg South Africa

Esther T. Akinlabi
Pan African University for Life and Earth Sciences Institute (PAULESI), Ibadan, Nigeria

Research Article

Keywords: Carbonized eggshells, Fly ash, Machinability, Optimization, Taguchi based grey relational analysis

Posted Date: May 5th, 2021

DOI: https://doi.org/10.21203/rs.3.rs-473917/v1

Characterization, machinability studies and multi-response optimization of AA 6082 hybrid metal matrix composite

Ndudim H. Ononiwu[12*], Chigbogu G. Ozoegwu[12], Nkosinathi Madushele[1], and Esther T. Akinlabi[3]

[1] Department of Mechanical Engineering and Science, University of Johannesburg South Africa
[2] Department of Mechanical Engineering, University of Nigeria Nsukka Nigeria
[3] Pan African University for Life and Earth Sciences Institute (PAULESI), Ibadan, Nigeria

Corresponding author*: 219122653@student.uj.ac.za, ndudim.ononiwu@unn.edu.ng

Abstract

This work investigated the effect of carbonized eggshell and fly ash on the microstructure, mechanical properties and machinability of AA 6082. The fabrication method selected for this study was stir casting. For the hybrid metal matrix composite, the weight fraction was 2.5wt% carbonized eggshell and 2.5wt% fly ash. The microstructural examination of the cast composite showed an even dispersal of the reinforcing phases in the aluminium matrix. Density analysis saw a 10.66% reduction of the cast composite in comparison to the aluminium alloy. Improvements of 12.32%, 21.91%, and 8.30% were recorded for the microhardness, tensile strength and compressive strength respectively. The wear studies of the cast samples revealed coefficients of friction (CoF) of 0.499 and 0.290 for the base metal and the AMC respectively. For the machinability studies, the surface roughness and flank tool wear were the responses under consideration. The design of experiments was conducted using the Taguchi method. The input parameters for this investigation was the cutting speeds (100 mm/min, 200 mm/min, 300 mm/min), feeds (0.1 mm/rev, 0.2 mm/rev, 0.3 mm/rev) and depths of cut (0.5 mm, 1.0 mm, 1.5 mm). For the multi-response optimization, Taguchi based grey relational analysis was used. The analysis of variance (ANOVA) of the grey relational grade (GRG) revealed that the feed was the most influential factor on the surface roughness and tool wear. The initial optimization showed the optimal cutting speed, feed and depth of cut as 200 mm/min, 0.2 mm/rev and 1.5 mm respectively. The confirmatory experiments revealed that the optimal combination of factors was 200mm/min, 0.2 mm/rev and 0.5 mm for the cutting speed, feed and depth of cut respectively.

Keyword: Carbonized eggshells; Fly ash; Machinability; Optimization; Taguchi based grey relational analysis

1.0 Introduction

Metal matrix composites (MMCs) have continued to receive adequate attention due to the prospects of improved overall properties making them easily applicable across several industrial sectors not limited to automobiles, aerospace, military, marine and structural applications. These composites are already poised to replace conventional materials for the purpose already stated. Among the applicable base metals for MMC fabrication, aluminium has received numerous attention because of its lightweight,

corrosion resistance, and adequate strength-to-weight ratio [1]. Research into the fabrication of aluminium matrix composites (AMCs) has yielded noteworthy improvements in the properties under investigation such as research done by Ikumapayi et al [2] to study the effects of coconut shell ash, cow bone ash and palm kernel ash on corrosion resistance of AA 7075. The results indicate that reinforcing the aluminium alloy with palm kernel shell ash produced the AMC with the least corrosion resistance. Research done by Rao et al [3] reported refined grain structure, reduction of destiny, and improvements of the hardness and tensile strength of AA 6061 reinforced with particulate fly ash in comparison to the base metal. Kurapati and Kommineni [4] reported improvements in the wear behaviour of hybrid AA 2024/fly ash/SiC in comparison to the monolithic metal due to adequate distribution of the reinforcing particulates.

Based on the required application, 8 major grades of aluminium alloys are available depending on the alloying elements. Among the aluminium grades available, AA 6082 is one of the commonly used. AA 6082 is a medium-strength aluminium alloy with good corrosion resistance. It is regarded as a structural alloy that has the best strength in the aluminium 6XXX series. It is used in transport, bridges, trusses and cranes among other application. This aluminium alloy possesses high machinability in the T6 and T651 temper [5]. The prospect of the application of AA 6082 for MMC applications has led to researches such as the one reported in [6] where AA 6082 reinforced with $CaCO_3$ was fabricated via friction stir processing. Improvements in microhardness and wear resistance in comparison to the base metal were reported. Via squeeze casting, Jiang et al [7] reinforced AA 6082 with SiC. The investigation into the microstructure and mechanical properties reported grain refinement brought about by the addition of the SiC particles. It was also reported that the addition of SiC brought about 10.73%, 72.7%, 193.9%, 23.5% and 25.2% improvements of the tensile strength, yield strength, ductility, modulus of elasticity and hardness respectively. Kumar et al [8] characterized and investigated the mechanical properties of AA 6082 reinforced with ZrO_2 and coconut shell. The investigation suggested that the introduction of the hybrid reinforcements was capable of producing lightweight engineering materials as evidenced by the reduction of the density of the fabricated MMC. There were improvements in the hardness, tensile strength and flexural strength while the impact strength of the MMCs decreased with increasing proportions of the reinforcements.

Machinability is usually defined based on indices which includes the surface roughness, tool wear, cutting forces, cutting temperature, material removal rate (MMR) among others. The machinability of a material describes the ease with which a workpiece can be cut [9]. Part of the research into the machinability of MMCs is the need for optimization of certain input parameters such as cutting speed, feed, depth of cut, reinforcements weight fraction, tool nose radius among others. The need for optimization is necessary to effectively reduce machining cost, waste and ultimately maximize profit. Certain optimization techniques have been applied to machinability studies of AMCs. Such techniques are illustrated in fig.1.

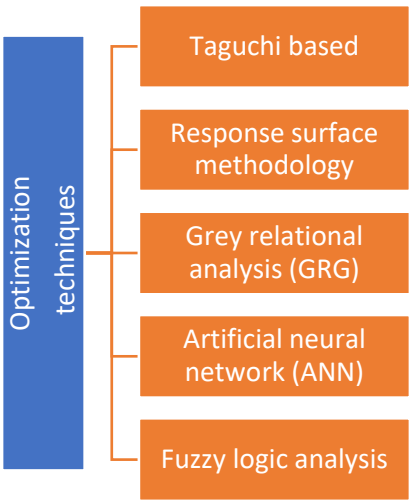

Fig 1 Optimization techniques applied for the machinability studies of AMCs

The versatility of these optimization techniques has resulted in their application into other aspects of MMC research including fabrication and tribology optimization [10], [11]. Of these optimization techniques specified in fig.1, the Taguchi optimization technique is well applied in MMC machinability analysis owing to its simplicity and its ability for process improvement. The major shortcoming of the Taguchi method of optimization is its inability to optimize multi-responses [12]–[15]. Research into the machinability studies of selected AMCs include those done by [16] which investigated the effect of bismuth on the surface roughness and cutting forces on Al-Mg_2Si. The dry turning test considered the variation of the cutting speed and feed. The results of the study disclosed that the surface roughness and cutting forces decreased with increasing weight fraction of bismuth. Jiang et al [17] investigated the effect of TiB_2 on the machinability of AA 7050. The results of the investigation indicated that the surface roughness decreased with increasing cutting speed while increasing the feed decreased the surface integrity of the AMC. Pugazhenthi [18] investigated the machinability of AA7075/TiB_2 while varying the cutting speed, feed, depth of cut and weight fraction of TiB_2. The machinability indices under investigation were the cutting forces and surface roughness. It was reported that the surface roughness decreased with increasing cutting speed and TiB_2 proportion while increasing the feed and depth of cut caused an increase in the cutting force. The AVOVA results indicate that the TiB_2 reinforcements were the highest contributor to the cutting forces and surface roughness. Results reported in [19] indicated that the feed has the most influence on the surface roughness of AA 6061 reinforced with rock dust. [20] investigated the effect of the cutting speed, feed and depth of cut on the surface roughness, temperature, flank tool wear and material removal rate of AA 7075/SiC composite. The results indicate that the feed, which the ANOVA analysis showed, has the greatest effect on the investigated responses.

Most research efforts including those reviewed here focused on characterization and/or machinability of AMCs fabricated with either synthetic reinforcements or a combination of synthetic reinforcements and sustainable reinforcement. This work involves the examination of the effect of two sustainable reinforcement materials, Fly ash and carbonized eggshell, on the microstructure, mechanical properties, tribology and machinability of AA 6082. Therefore, the basis for the novelty of this work is the study of an innovative sustainable material via comprehensiveness experimental characterization of the physical,

microstructural, mechanical and machinability properties including the machinability optimization of the new material.

2.0 Material and methods

2.1 Composites fabrication

The elemental composition AA 6082 used as the matrix material is shown in table 1. Stir casting was selected as the processing route for the fabrication of the composites. This processing route was preferred because of its ease and cost-effectiveness [21].

Table 1 Elemental composition of the metal matrix

Composition	Si	Fe	Cu	Mn	Mg	Cr	Ni	Ti	Al
%	0.898	0.535	0.079	0.593	0.142	0.055	0.108`	0.013	Bal

The AA 6082 matrix was sourced as sheets from Metal Centre Johannesburg. The as-received sheets were cut and weighed based on the designed weight fractions depicted in table 2. The type C fly ash was sourced from Ash resources Johannesburg, while the eggshells were sourced from restaurants located in the University of Johannesburg, Auckland Park Campus. The eggshells were cleaned and sundried to eliminate any organic matter. The eggshells were subsequently dried in an electric oven for 2 days to remove any remaining moisture due to possibly humid conditions. This step was also taken for the fly ash. The stirrer and steel die were preheated to 350°C±20°C. This was done to avoid the effect of the temperature difference between the stirrer and the molten matrix and to ensure uniform fluidity and solidification of the cast. For the graphite crucible, it was preheated to a temperature of 600°C to avoid cracks that could occur as a result of thermal shock. Both reinforcements were charged into a muffle furnace and preheated at a temperature of 300°C for 1 hour to ensure adequate wettability between the reinforcements and the matrix. The temperature of the furnace was increased to 760°C±5°C to initiate the melting process for the aluminium alloy. 1wt% magnesium was charged into the crucible after the removal of slag and subsequent introduction of the preheated reinforcements to ensure proper wettability and improve the interfacial bonding between the reinforcing phases and the aluminium matrix [21],[22]. The stirring was done to ensure that the less dense reinforcements mix properly in the molten matrix to promote uniform dispersal. The stirring was done for 10 minutes before casting commenced.

Table 2 Proportions of the cast samples

Composition	Al(wt%)	Carbonized eggshells (wt%)	Fly ash (wt%)
AA 6082	100	-	-
AA 6082 + CES + FA	95	2.5	2.5

2.2 Microstructural examination

The microstructure of the cast composite was investigated using the TESCAN model type VEGA LMH. This equipment was also used to study the elemental composition of the cast composite via energy dispersive spectroscopy (EDS). The metallographic analysis was done to investigate the level of distribution of the hybrid dispersed phases in the aluminium matrix and also to check for the presence of defects usually in the form of voids, agglomerations and segregation of the reinforcing particulates.

2.3 Mechanical properties and density

This study also attempted to study the effect of the hybrid reinforcements on selected mechanical properties including compressive strength, tensile strength, ductility and microhardness. The tensile strength and ductility of the samples were obtained via the MKS Universal tensile testing machine with a frame capacity of 1000KN as per the ASTM E8 standard. In the case of the compressive strength, the utilized equipment was the Zwick/Roell Universal tensile testing machine with a maximum applicable load of 250KN. The dimension of the selected samples was 2mm X 2mm as per the ASTM standards. As in the case of the tensile strength test, 3 replicates were prepared for each sample for reproducibility of the results. The hardness test was conducted using the Times Vickers hardness tester which is equipped with a diamond cone indenter. The applied test force was 300 gF with a dwell time of 15 secs per indentation. 5 indentations 1mm apart were produced for each sample was and the average recorded as the obtained values for the microhardness. All the mechanical tests were done at 23°C (room). The experimental density of the cast samples was obtained via the Archimedes principle.

2.4 Wear studies

The wear study was conducted to investigate the effect of the carbonized eggshell and fly ash hybrid reinforcements on the aluminium matrix in comparison with the unreinforced aluminium alloy. The wear study was conducted using the Antom Paar ball-on-disc tribometer shown in fig.2. The selected load was 10N while the linear speed was 36.04 cm/s. The sliding distance was 440 m. The selected ball for the study was an alumina ball of 6mm diameter.

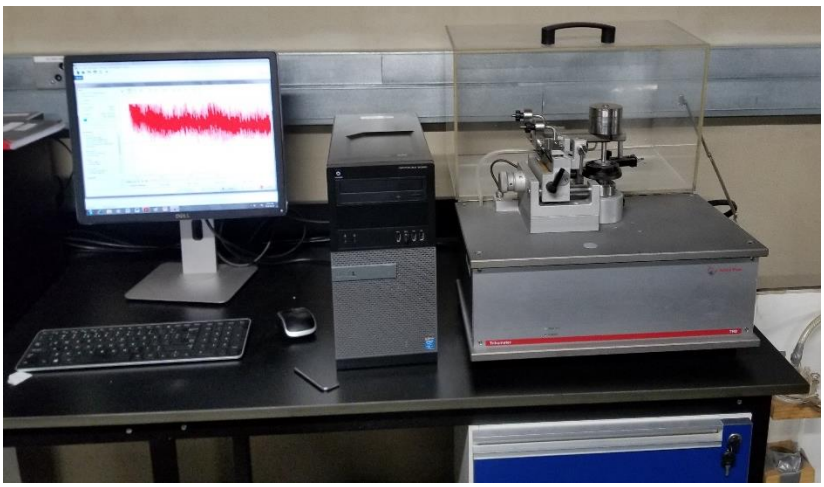

Fig 2 Antom Paar ball-on-disc tribometer

2.5 Machinability tests

The machinability investigation was undertaken to understand the effect of the hybrid reinforcement on the machinability of the AA 6082 hybrid composite. Joel et al and Nicholls et al [23], [24]that the inclusion of reinforcements into aluminium matrix ultimately decreases its machinability. To this effect, this work expressly investigated the machinability of the cast hybrid to determine the reinforcement's effect while conducting optimization of the selected input parameters. The machinability indices under investigation were the surface roughness and the flank tool wear. The machine tool used for the

machinability studies was the Ecoline ctx 3 axis CNC lathe. The specifications of the machine tool are summarized in table 3.

Table 3 Specifications of the Ecoline ctx 3 axis CNC machine tool

Turntable diameter	**200 mm**
Turning length	455 mm
Spindle bore	51 mm
Machine tool dimension	4228 X 3115 X 2153 mm
Weight	3800 Kg
Clamping chuck diameter	210 mm
Spindle speed	1 to 5000rpm/min

A dry turning operation was selected for the investigation. The cast workpiece had a dimension of 67mm X 200mm. The need to provide a reference surface roughness state was responsible for an initial rough cut on the workpiece. A Korloy carbide single-point cutting tool inserts with a nose radius of 0.4 mm was selected for the metal cutting process. The surface roughness was analysed using the Mitutoyo SJ-201 (0.25 X 5) portable surface roughness tester equipped with a diamond cone stylus which was responsible for taking precise mean surface roughness (Ra) values. At the end of each run, the 3 points along the cast workpiece were measured and the mean surface roughness was recorded. The average flank tool wear (VBB) was analysed using the SEM. At the end of each run, the insert used was changed and stored to measure the tool wear via the scanning electron microscope. The stated equipment for the machinability studies is depicted in fig.3.

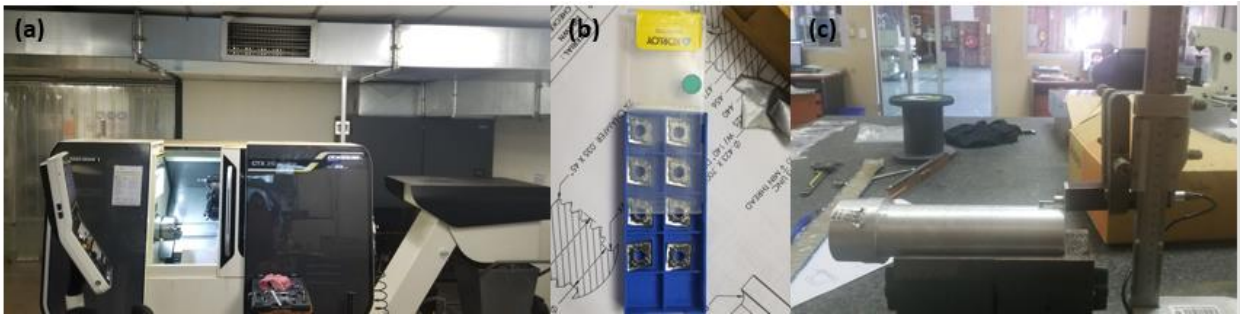

Fig 3 Equipment used to carry out the machinability analysis (a) CNC machine tool (b) Korloy single point cutting tool insert (c) Surface roughness tester

2.6 Taguchi Design of experiments and optimization

The design of experiments (DOE) was conducted via the MINITAB 17 statistical software. The independent variables under consideration for this study were the cutting speed, feed and depth of cut. The process parameters are summarized in table 4. The L_9 orthogonal array DOE selected for this investigation considers 3 process parameters without interaction to be varied at 3 discrete levels. This L_9 orthogonal array was designed to run 9 individual experiments to evaluate the tool wear and the surface roughness of the cutting tool inserts and the AA 6082/FA/CES AMC respectively.

Table 4 Control factors of the responses and their levels

				Levels		
S/No	Factors	Designation	Units	1	2	3
1	Cutting speed	v	mm/min	100	200	300
2	Feed	f	mm/rev	0.1	0.2	0.3
3	Depth of cut	d	mm	0.5	1	1.5

Optimization of the responses was done using the signal to noise ratio (S/N) analysis. The S/N analysis is a tool used in the Taguchi response optimization process to ascertain the robustness of the process and evaluate any deviation from the desired values [25]. In this optimization method, greater values of S/N ratios are usually preferred to reduce the effect of uncontrollable factors, and noise reduction. For this study, the smaller-the-better S/N ratio criterion was used to optimize the tool wear and surface roughness while the larger-the-better S/N criterion was used to optimize the Grey relational grade (GRG). The S/N ratio formulas for the smaller-the-better and larger-the-better criteria are depicted in equations 1 and 2 respectively.

$$\mathrm{S/N\ ratio} = -10\log\left(\frac{1}{n}\sum_{i=1}^{n} y_i^2\right) \qquad (1)$$

$$\mathrm{S/N\ ratio} = -10\log\left(\frac{1}{n}\sum_{i=1}^{n} \frac{1}{y_i^2}\right) \qquad (2)$$

Where i is the number of experiments conducted, y_i is the result of the ith experiment.

2.7 Grey relational analysis (GRA)

The use of Taguchi based approach for the optimization of responses has the weakness of being able to only optimize one response at a time. This reason has led to research into combining grey relational analysis with Taguchi based optimization technique. This combination has led to the hybridization of the Taguchi based-grey relational analysis which is capable of optimizing multiple responses [12]. The integration of grey relational analysis with the Taguchi based optimization works by converting multi-optimization problems into a single objective optimization problem [19]. This is done in a series of steps. The 1st step is to normalise the data using the expression shown in equation 3. This equation was selected since the aim of the response processing was to reduce both the flank tool wear and surface roughness.

$$Y_{ij} = \frac{(\max(z_{ij}) - (z_{ij}))}{\max(z_{ij}) - \min(z_{ij})} \qquad (3)$$

Where z_{ij} is the experimental result obtained for the jth experiment, $\max(z_{ij})$ is the maximum value of obtained experimental results obtained from the L_9 Taguchi design and and $\min(z_{ij})$ is the minimum value of the experimental results gotten from the L_9 Taguchi design.

The next step is the obtain the deviation sequence which is done using equation 4.

$$\Delta_{ij} = \max(Y_{ij}) - Y_{ij} \qquad (4)$$

Where Δ_{ij} is the deviation sequence, $\max(Y_{ij})$ is the maximum normalized value and Y_{ij} is the reference normalized value.

With the value of the deviation sequence, the grey relational coefficient (GRC) of the individual responses is calculated using equation 5.

$$GRC_{ij} = \frac{(\Delta_{min} + \delta\Delta_{max})}{(\Delta_{ij} + \delta\Delta_{max})} \quad (5)$$

Where Δ_{min} is the minimum deviation sequence, Δ_{max} is the maximum deviation sequence and δ is the identification coefficient which is defined to be usually set at 0.5 to assign equal weight to each parameter.

The grey relational grade (GRG) is eventually used as a representation of the two responses in the Taguchi optimization. It is obtained via equation 6 as;

$$GRG_{ij} = \frac{1}{n}\sum_{1=1}^{n} GRC_{ij} \quad (6)$$

3.0 Results and discussion

3.1 Mechanical properties, and density

The summary of the results for the density and the investigated mechanical properties are displayed in table 5. The analysis of the microhardness revealed a 12.23% increase in comparison to the base metal. The enhancement of the microhardness is a result of the presence of the hard-reinforcing hybrid particles which work to resist the relative motion between individual grains for any given load applied.

Table 5 Summary of the density and mechanical properties of the cast samples

Sample	Density (g/cm^3)	Microhardness (HV)	Tensile strength (MPa)	% Elongation	Compressive strength (MPa)
AA6082	2.72	63.23	141.60	8.50	121.23
AA6082/FA/CES	2.43	71.02	172.63	2.62	131.29

The tensile strength of the cast composite improved by 21.9%. In addition to the uniform dispersal of the fly ash and carbonized eggshell particles, the improvement in tensile strength is brought about by transferring the load from the aluminium matrix to the hybrid reinforcements due to their different elastic constants [26]. The reduction in ductility which has also been reported in [27], [28] was also reported in this investigation as being a result of the reinforcing phases present in the aluminium matrix. In the fabrication of the composite, there is usually a trade-off between tensile strength and ductility. The compressive strength of the composite was generally improved by adding the hybrid reinforcements. This improvement is due to the ability of the reinforcements to resist deformation when compressive forces are applied [29].

3.2 Microstructure

The micrograph of the AMC under consideration as shown in fig.4 shows evidence of uniform dispersal of the hybrid reinforcements in the aluminium matrix. There was no discernible presence of

agglomeration or segregation of the reinforcements. This is primarily due to adequate stirring of the melt before casting. There was also no visible presence of pores in the microstructure. This in addition to proper stirring is due to the presence of inert gases being charged into the melt before casting. It is also due to the preheating of the steel mould which ensured uniform flow and solidification during casting. The Energy dispersive spectroscopy (EDS) analysis of the hybrid sample shown in fig.5 revealed peaks of aluminium, oxygen, carbon, silicon and manganese.

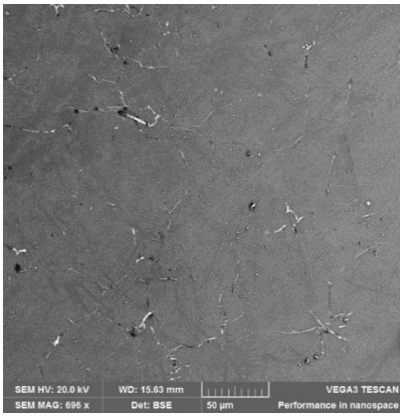

Fig. 4 SEM micrographs of AA 6082/FA/CES

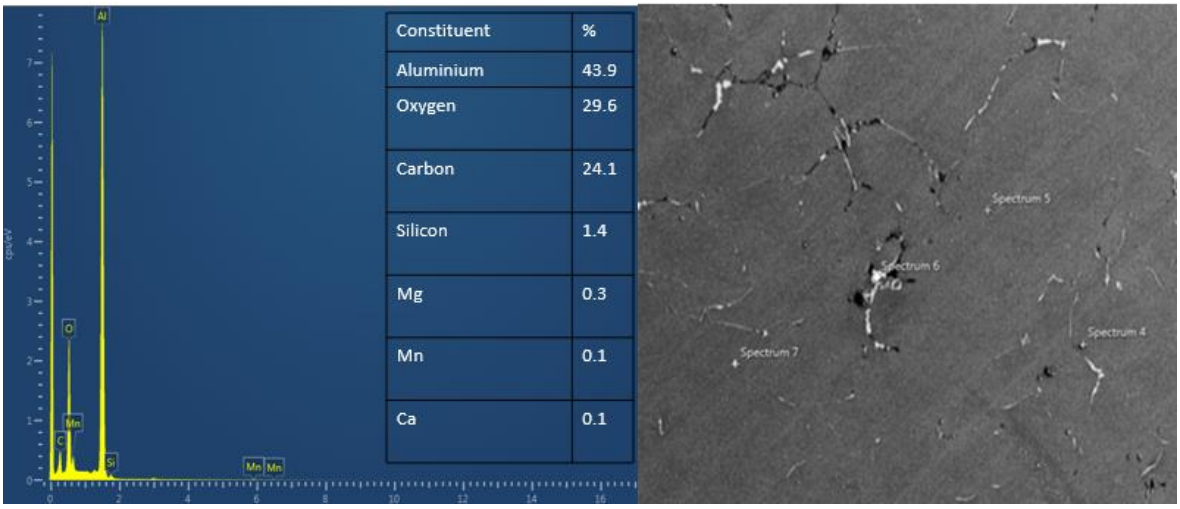

Constituent	%
Aluminium	43.9
Oxygen	29.6
Carbon	24.1
Silicon	1.4
Mg	0.3
Mn	0.1
Ca	0.1

Fig. 5 EDS analysis of AA6082/FA/CES

3.3 Tribology studies

The wear resistance study was conducted based on the coefficient of friction analysis. The results are summarized in fig.6. From these results, it is shown that the cast composite exhibits higher wear-resistant properties due to the relatively lower coefficient of friction in contrast to the matrix. The average CoF of the base metal and composite are 0.499 and 0.29 respectively. It is shown that the CoF of the AMC is lower than that of the matrix which indicates improved wear resistance. The improved wear resistance is because of the hard-reinforcing particles which work to resist the relative motion of the alumina ball on the surface of the cast hybrid composite samples. The reduction of the CoF with increasing sliding distance could be due to the transition of the wear mechanism from adhesive to

abrasive. From the results, it is shown that the CoF for both samples decreased with increasing sliding distance. This could be attributed to the Al_2O_3 formation on the surface of the cast samples which acts as a lubricating film thereby reducing the effect of friction [30]. The formation of the oxide layer forms a barrier that reduces the contact between the alumina ball and the aluminium counter face thereby improving the wear resistance of both samples under consideration. Another reason for the improved wear resistance of the cast AMC is the adequate interfacial bonding between the hybrid reinforcements and the aluminium matrix which resists the pull-out of the hybrid reinforcements during the relative movement between the ball and the counter face [31].

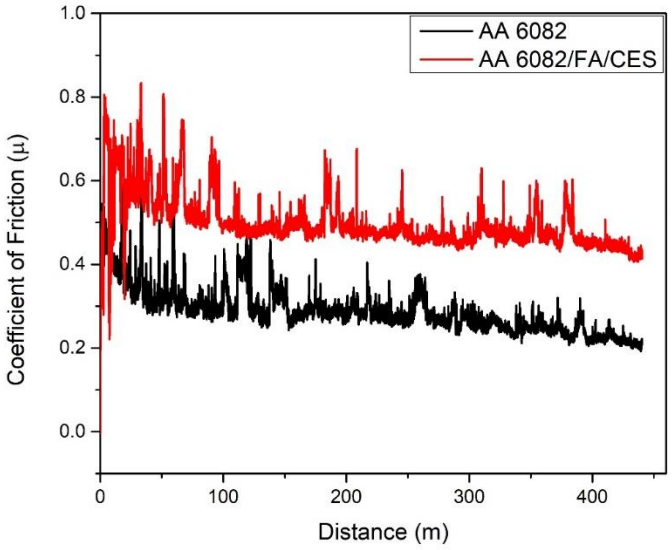

Fig. 6 Coefficient of friction for the matrix and hybrid AMC

The analysis of the wear tracks as seen in fig.7 obtained with the aid of SEM shows the presence of predominantly abrasive wear evident by the presence of grooves and delamination. There was also the presence of adhesive wear as confirmed by the presence of aluminium debris deposited on the surface of the cast samples. The presence of abrasive wear in both samples is evident by the presence of grooves formed as the ball moves along the face of the cast samples due to the application of the normal load. The movement of the alumina ball along the surface of the cast samples led to a rise in temperature which aids the plastic deformation of the counterface. The wear debris indicated in the wear mechanism analysis is a result of the cutting of the deformed aluminium which stuck to the alumina ball. Both the aluminium and the cast hybrid AMC have similar wear mechanisms regardless of the difference in CoF.

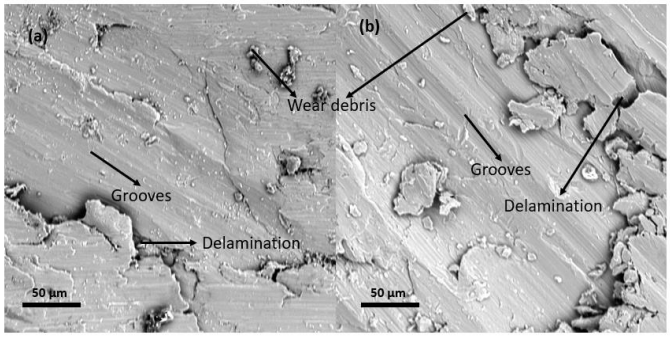

Fig. 7 Micrographs of the wear mechanism for (a) AA 6082 (b) AA 6082/FA/CES

3.4 Design of experiments

Using the Taguchi DOE, 9 distinct experiments were developed from the L_9 orthogonal array. These experiments were designed using the MINITAB 17 statistical analysis software. The experiments were conducted based on the designed experiments to obtain the tool wear of the carbide tool inserts and the surface roughness of the AA 6082/FA/CES hybrid composite. The L_9 orthogonal array is shown in table 6.

Table 6 L_9 Orthogonal array and results

Runs	Cutting Speed	Feed	Depth of cut	Tool wear (µm)	Surface Roughness (µm)
1	100	0.1	0.5	23.39	2.07
2	100	0.2	1	54.05	1.68
3	100	0.3	1.5	320.36	2.31
4	200	0.1	1	135.87	1.44
5	200	0.2	1.5	145.39	1.26
6	200	0.3	0.5	137.4	1.48
7	300	0.1	1.5	428.66	1.79
8	300	0.2	0.5	116.91	1.46
9	300	0.3	1	535.26	1.99

3.5 ANOVA

The analysis of variance (ANOVA) is a statistical tool utilised for different applications to determine the significance of 2 or more independent variables as they affect the response or group of responses. For this study, the ANOVA of the individual responses (tool wear and surface roughness) and the grey relational grades obtained through the utilization of equations (3)-(6) are shown in table 7, 8 and 9. This was done to determine the significance of the input parameters on the associated response(s).

Table 7 ANOVA for tool wear

Source	DF	Seq SS	Contribution (%)	Adj SS	Adj MS	F-Value	P-Value
Cutting speed	2	100604	40.48	100604	50302	34.32	0.028
Feed	2	77304	31.1	77304	38652	26.37	0.037
Depth of cut	2	67690	27.24	67690	33845	23.09	0.042
Error	2	2932	1.18	2932	1466		
Total	8	248530		S=38.2864	R^2=98.82%	R^2adj=95.58%	

Table 8 ANOVA for surface roughness

Source	DF	Seq SS	Contribution (%)	Adj SS	Adj MS	F-Value	P-Value
Cutting speed	2	0.59227	61.36	0.59227	0.29613	24.61	0.039
Feed	2	0.3272	33.90	0.3272	0.1636	13.6	0.069
Depth of cut	2	0.02167	2.24	0.02167	0.01083	0.9	0.526
Error	2	0.02407	2.24	0.02407	0.01203		
Total	8	0.9652	100	S=0.109697	R^2=97.53%	R^2adj=90.03%	

The ANOVA analysis of the tool wear indicates that all the independent variables have p-values < 0.05 which indicates that they all have a significant effect on the cutting tool wear while machining the cast hybrid AMC. Further analysis of the significance of the independent variables on the tool wear indicates that the cutting speed has the most contribution of 40.48% on the tool wear. The feed and DoC have contributions of 31.10% and 27.24%. The ANOVA of the surface roughness also revealed that the cutting speed has the highest contribution of 61.36%. This result is in tune with research done by [32],[33]. The p-values of all the factors were 0.039, 0.069 and 0.526 for the cutting speed, feed and depth of cut respectively. These p-values as in the case of the ANOVA analysis of the tool wear indicates that the cutting speed is the significant factor that influences the surface roughness of the AA6082/FA/CES composite. The percentage contribution of the feed was 33.90% which also indicates that the feed is a major contributor to the surface roughness. The DoC had a contribution of 2.24% indicating little to negligible contribution on the surface roughness.

The ANOVA of the Grey relational grade was also conducted to investigate the effect of the cutting speed, feed and DoC on the tool wear and surface roughness. The p-values of the independent variables were all less than 0.05 indicating their significance on both the tool wear and surface roughness. In the case of the contribution of the factors on the GRG, the feed had a contribution of 48.12%, while the cutting speed and DoC have contributions of 36.79% and 14.77% respectively. The AVOVA analysis revealed that the feed has the most influence on the combined responses on the AA6082/FA/CES hybrid composite.

Table 9 ANOVA for GRG

Source	DF	Seq SS	Contribution (%)	Adj SS	Adj MS	F-Value	P-Value
Cutting speed	2	0.085551	36.79	0.085551	0.042776	114.75	0.009
Feed	2	0.111896	48.12	0.111896	0.055948	150.08	0.007
Depth of cut	2	0.034338	14.77	0.034338	0.017169	46.06	0.021
Error	2	0.000746	0.32	0.000746	0.000373		
Total	8	0.23253	100	S=0.109697	R^2=97.53%	R^2adj=90.03%	

3.6 Single-objective optimization

For both responses (tool wear and surface roughness), the experimental data were converted to the S/N ratio. Also, for both responses, the most influential independent variables were identified via the generated response table of the S/N ratio shown in table 10 and 11. Since a single objective for both the tool wear and surface roughness was to be minimized, the smaller-the-better criterion was utilized.

Table 10 Response table for Surface roughness S/N ratio

Level	Cutting speed	Feed	Depth of cut
1	-6.033	-4.848	-4.337
2	-2.860	-3.267	-4.550
3	-4.774	-5.552	-4.779
Delta	3.173	2.285	0.442
Rank	1	2	3

The delta statistics for the surface roughness depicted in table 10 shows the ranks of the individual responses based on the S/N ratios obtained via the Taguchi orthogonal array. The analysis showed that the cutting speed was assigned a rank of 1 with a delta value of 3.173 signifying that it is the predominant factor that affects the surface roughness of the cast composite. The feed and the depth of cut were assigned second (2.285) and third (0.442) ranks respectively. The result is in tune with fig.8 which shows the main effects plot for the S/N ratio for the surface roughness. The main effect plot indicates that the optimal combination of the factors to minimize the surface roughness of the AA6082/FA/CES hybrid composite are 200 mm/min for the cutting speed, 0.2 mm/rev for the feed and 0.5 mm for the depth of cut. The surface roughness decreases steadily with an increase in the depth of cut. This could be owing to an increase in chatter produced due to the vibration of the workpiece caused by cutting through larger sections of the workpiece. The increased surface roughness could also be due to either the pull out of the harder reinforcing particles or the migration of the particles as a result of increased heat generation during the cutting operation. The surface roughness decreases with an increase in cutting speed thereby improving the surface integrity of the cast AMC. Increased cutting speed improves the surface roughness of the cast composites due to lesser generation of built-up edges during cutting [34]. At lower cutting speeds, the fracture of the chips generated increases the surface roughness of the workpiece.

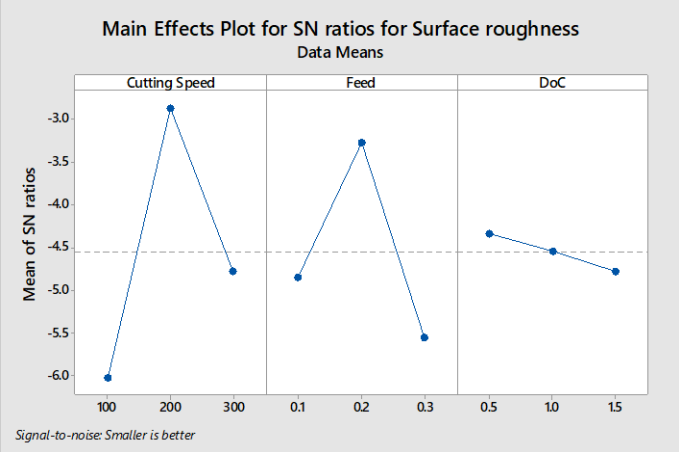

Fig. 8 Main effects plots for S/N ratio of surface roughness

The response table for the S/N ratio for the optimization of the tool wear is depicted in table 11. The table shows that the cutting speed as in the case of the surface roughness S/N ratio analysis had the rank of 1. This also suggests that it is the predominant factor that affects the cutting tool wear.

Table 11 Response table for Tool wear S/N ratio

Level	Speed	Feed	Depth of cut
1	-37.38	-40.90	-37.17
2	-42.89	-39.75	-43.96
3	-49.52	-49.15	-48.67
Delta	12.14	9.39	11.50
Rank	1	3	2

The depth of cut is ranked 2nd while the feed is ranked 3rd. The delta values of the independent factors are shown in the response table for the S/N ratio of the tool wear. The table also suggests that for the cutting speed, feed and depth of cut, levels 1, 2 and 1 respectively have the maximum S/N ratio which makes them the optimal S/N ratio for the optimization of the tool wear. This is further validated by the main effects plot for the S/N ratio of the tool wear depicted in fig.9. Based on the plot, the optimum combination of the factors is 100 mm/min, 0.2 mm/rev and 0.5 mm. The main effects plot for the S/N ratio of the tool wear shows that the flank tool wear of the carbide inserts increased with increasing cutting speeds. This is in tune with research conducted by [35]. It was suggested that this could be owing to the tool's contact with the hard-reinforcing particles, increased generation of heat during cutting due to friction between the workpiece and the tool.

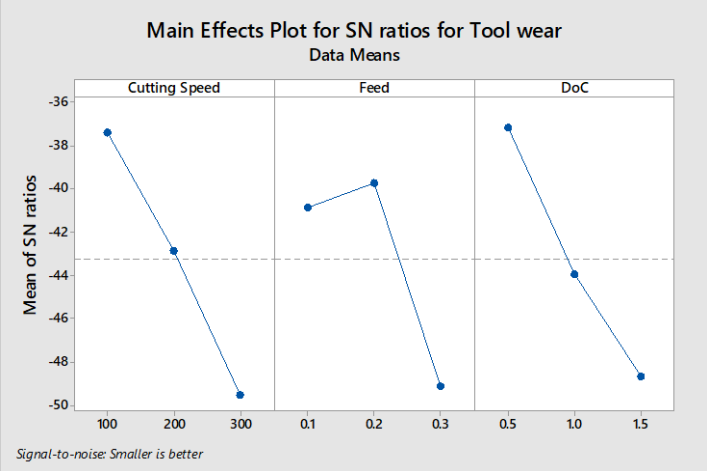

Fig. 9 Main effects plots for S/N ratio of tool wear

3.7 Multi-objective optimization

The Taguchi based- grey relational analysis was employed to perform the multi-objective optimization of the cutting tool flank wear and surface roughness of the cast AMC. The 'larger the better' criterion was selected because the objective of the study was to maximize the GRG. The results obtained from experimental data provided in table 6 were processed to obtain the grey relational grade populated in table 12. The methodology for processing the experimental data obtained via the L_9 orthogonal array design of experiments has been described.

Table 12 Response table for S/N ratio for grey relational grade

Level	Speed	Feed	Depth of cut
1	-4.647	-4.361	-3.005
2	-2.502	-2.362	-4.720
3	-6.113	-6.540	-5.538
Delta	3.611	4.178	2.533
Rank	2	1	3

The response table for the S/N ratio tabulated in table 13 was used to initiate the optimization of the input parameters. The response table indicated that the feed was the predominant factor influencing the responses under investigation and was ranked 1st. The cutting speed and depth of cut were ranked 2nd and 3rd respectively. Further analysis of the response table for the S/N ratio indicated that level 2, level 2 and level 1 for the cutting speed, feed and depth of cut respectively were the combinations of optimum factors for maximizing the grey relational grade and by extension optimizing the surface roughness and tool wear. This is also evident in the main effect plot of the S/N ratio of the GRG depicted in fig.10. The S/N ratio of the experiments obtained via the Taguchi process indicates that experimental run 5 which combined the factors of 200 mm/min, 0.2 mm/rev, and 1.5 mm/rev gave the maximum S/N ratio for the GRG as -1.529. The grey relational analysis also confirmed experimental run 5 as the initial optimum combination as it was assigned the grey relational rank of 1.

Table 13 Ranks of grey relational grade and S/N ratios

Runs	Cutting Speed	Feed	Depth of cut	GRG	S/N ratio	Rank
1	100	0.1	0.5	0.6966292	-3.139966	6
2	100	0.2	1	0.7242877	-2.801778	3
3	100	0.3	1.5	0.3981124	-7.999886	8
4	200	0.1	1	0.7196865	-2.857133	4
5	200	0.2	1.5	0.8385966	-1.528938	1
6	200	0.3	0.5	0.6982585	-3.119675	5
7	300	0.1	1.5	0.442352	-7.084641	7
8	300	0.2	0.5	0.7282606	-2.754264	2
9	300	0.3	1	0.37583	-8.500171	9

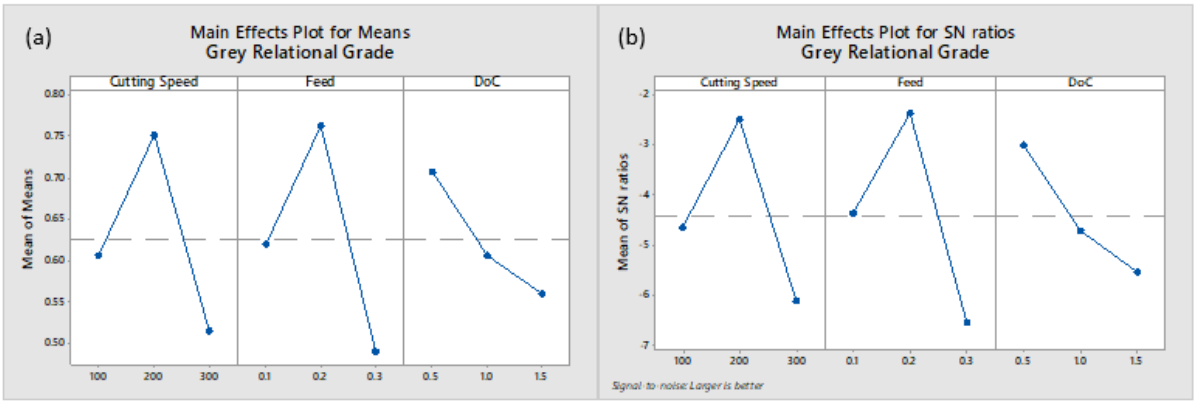

Fig. 10 (a) Main effects plot for means of GRG (b) Main effects plots for S/N ratio of GRG

3.8 Regression analysis

A regression model is used to make a correlation between the factors and the desired responses. The regression model used in the prediction for the effect of the cutting speed, feed and depth of cut on the flank tool wear and surface roughness was obtained using the 2nd order regression methodology. For this prediction situation, the 2nd order regression model was preferred because the R^2 value of the 1st order equation was 30.17% which was relatively low. As a result, the prediction gave GRG results with high absolute percentage error in comparison to the GRG obtained from the normalization of the experimental results of the tool wear and the surface roughness. The 2nd order regression model is shown in equation 7.

$$\mathrm{GRG} = -0.000023\mathrm{v}^2 - 24.65\mathrm{f}^2 + 0.008503\mathrm{v} + 9.288\mathrm{f} - 0.784\mathrm{d} - 0.005420\mathrm{vf} + 0.001517\mathrm{vd} + 1.392\mathrm{fd} - 0.3091 \qquad (7)$$

Where v is the cutting speed, f is the feed and d is the depth of cut.

The regression model developed with the use of the regression tool on Minitab 17 for the GRG was based on the identified independent variables. Based on this result, it can be deduced that the regression model is capable of predicting the effects of the selected independent variables on tool wear and surface roughness. Fig.11 a and b show the normal probability plots and the residuals versus fits of

the regression equation shown in equation 7 respectively. The comparison between the experimental data represented by the grey relational grade and the predicted values of the same response is depicted in fig.12. The results shown in the graphs show the closeness between the experimental and predicted results. The validity of the 2nd order regression model is also shown in the absolute error depicted in table 14.

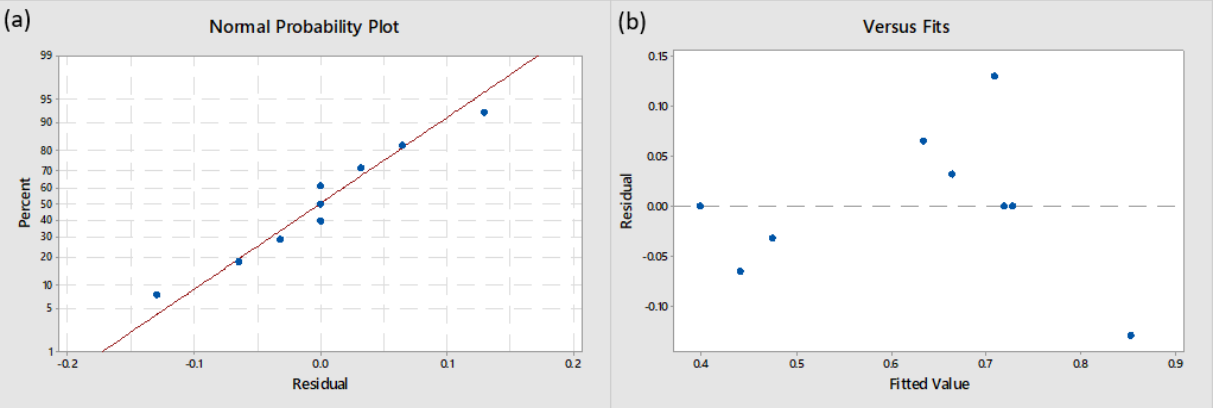

Fig. 11 (a) Normal probability plots (b) Residual vs fits plot for the developed 2nd order regression model

Table 14 Percentage error of the predicted Grey relational grade

GRG	GRG optimized	% Error
0.69663	0.69275	0.55685
0.72429	0.72050	0.52295
0.39811	0.39445	0.91994
0.71969	0.70400	2.17963
0.83860	0.82300	1.85984
0.69826	0.68270	2.22819
0.44235	0.40695	8.00312
0.72826	0.69295	4.84862
0.37583	0.34060	9.37392

The residual plots obtained from the regression model formulated to predict the effect of the factors on the multi-responses was undertaken to evaluate the integrity of the regression model depicted in equation 7. From the normal probability plots of the residuals, it is evident that the 9 data points are very close to the straight line which indicates that the error terms are normally distributed. Fig.11b shows the residual vs fit plots which is a scatter plot used to detect the non-linearity of the developed regression model. The residual versus fits indicates that the data points are symmetrically distributed as there are not any clear patterns.

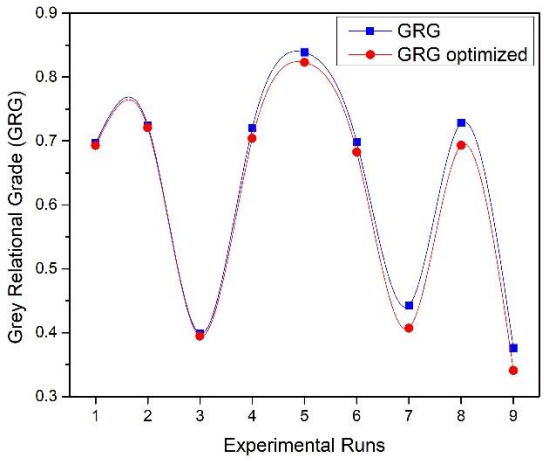

Fig. 12 Comparison between the actual and predicted GRG for the experimental runs

The contour plots depicted in fig.13 was used to see the effect of the predictor variables on the measured responses. The measured response for this analysis was the grey relational grade. The contour plots for the effects of the cutting speed and feed depicted in fig.13a shows that the maximum value of the GRG (greater than 0.7) was at cutting speeds of 132.56 mm/min and 259.69 mm/min and feed rate of 0.134 mm/rev and 0.25 mm/rev. The contour plots for the effect of the cutting speed and depth of cut on the GRG depicted in fig.13b revealed that the maximum region for the maximum GRG at cutting speed of 172.09 mm/min and 233.64 mm/min. However, for the depth of cut, the GRG is maximum at 1.36 mm and 1.50 mm. The relationship between the feed rate and the depth of cut represented in fig.13c showed that the GRG was maximum at a feed rate of between 0.167 mm/rev and 0.227 mm/rev while the depth of cut was maximum between 1.35 mm and 1.50 mm. The contour plots in general revealed that the maximum value of the grey relational grade which translates to improved surface roughness and tool wear is achieved at higher depth of cut and cutting speeds between 130 mm/min and 260 mm/min. As in the case of the cutting speed, the contour plots show no discernible trend unlike the depth of cut which improved with increased depth of cut, keeping the feed between 0.13mm/rev and 0.25mm/rev.

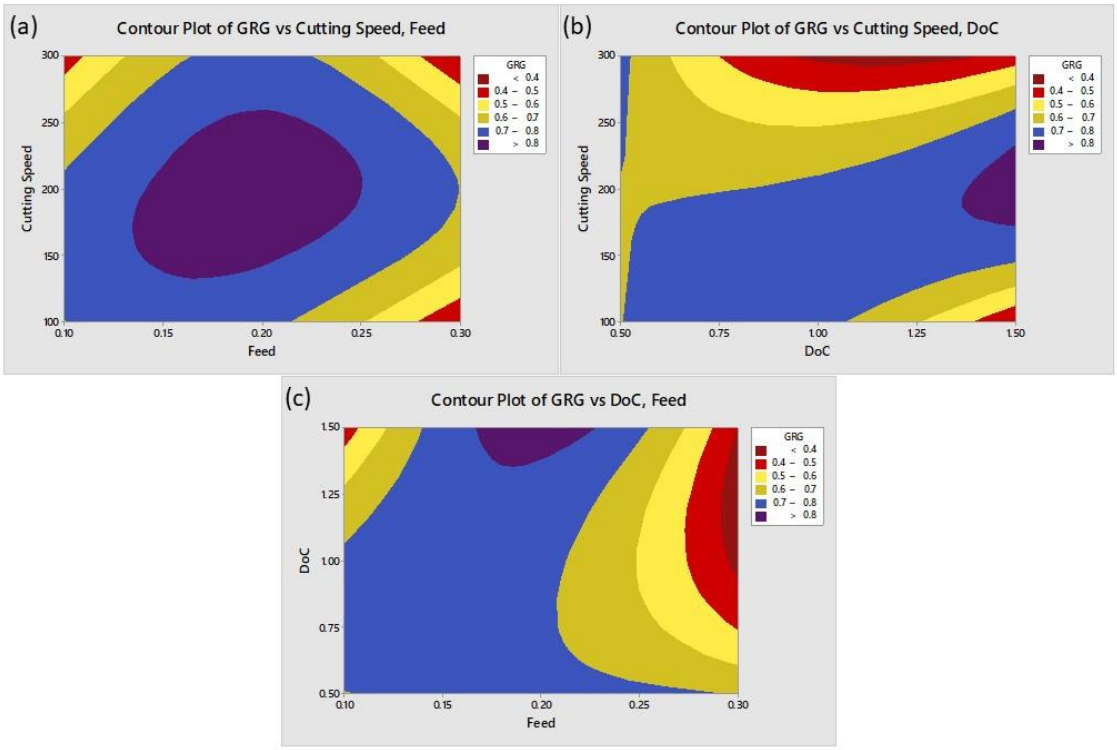

Fig. 13 Contour plots for Grey relation grade against (a) Cutting speed and feed (b) cutting speed and depth of cut (c) depth of cut and feed

3.9 Confirmation experiments

The Taguchi-grey relational analysis method was used to obtain the ideal combination of the investigated input parameters to optimize the cutting tool wear and surface roughness of the cast hybrid AMC. The last phase of the GRA is to verify the optimum condition for the multi-objective quality characteristics through confirmatory experiments [12]. The confirmation test was done using equation 8 to validate the multi-objective optimization process.

$$\beta = \beta_t + \sum_{i=0}^{n}(\beta_i - \beta_t) \qquad (8)$$

Where β_t is the total mean of the grey relational grade, and β_i is the average of the grey relational grade of the optimum factors.

The results of the confirmation of experiments identified level 2 for the cutting speed, level 2 for the feed and level 1 for the depth of cut which directly translates to 200 mm/min, 0.2 mm/rev and 0.5mm for the cutting speed, feed and depth of cut respectively. The calculated grey relational grade via equation 8 is 0.97428. This result established a 16.18% improvement in the grey relational grade. Table 15 summarizes the comparison between the initial and the optimum machining parameters.

Table 15 Results of the confirmation experiment

		Optimal Design parameters	
	Initial design parameters	Prediction	Experiment
Level	v2 f2 d3	v2 f2 d1	v2 f2 d1
Surface roughness	1.26		1.28
Tool wear	145.39		97.65
GRG	0.83860	0.97428	0.86920

Conclusion

From the investigation of the effect of fly ash and carbonized eggshells on the microstructure, density, mechanical properties and machinability of AA 6082, the following conclusions can be made.

1. The analysis of the microstructure revealed that the reinforcements were homogeneously dispersed in the aluminium matrix. The presence of the hybrid reinforcements was responsible for the decrease in the density from 2.72 g/cm^3 for the base metal to 2.43 g/cm^3 for the cast composite.
2. The studies of the mechanical properties revealed that the microhardness improved from 63.23 HV to 71.02 HV. The tensile strength improved from 141.60 MPa to 172.63 MPa while the compressive strength improved from 121.23 MPa to 131.29 MPa. The existence of the reinforcing particles in the aluminium matrix resulted in a decrease in the ductility of the composite from 8.5% for the base metal to 2.62%.
3. The wear studies showed an improvement in wear resistance evident from the reduction of the CoF in comparison to the base metal. The predominant wear mechanism for both samples was abrasive and adhesive wear.
4. The ANOVA analysis for the tool wear and surface roughness showed that the cutting speed was the most influential factor, while the feed was the most influential factor for the grey relational grade.
5. The single objective optimization of the individual responses showed that the optimal combination of factors was 200 mm/min, 0.2mm/min and 0.5 mm/min for the surface roughness, and 100mm/min, 0.2 mm/rev and 0.5 mm for the tool wear. The multi-objective optimization using the Taguchi based GR revealed the optimal combination of factors to be 200 mm/min, 0.2mm/min and 0.5 mm/min for the cutting speed, feed and depth of cut respectively.

Declarations section

Funding

No funding was received for conducting this study

Conflicts of interest

The authors have no conflicts of interest to declare that are relevant to the content of this article.

Availability of data and material

Not applicable

Code availability

Not applicable

Ethics approval

No data, theory or test from this work has been presented elsewhere. Proper acknowledgments to other work have been made.

Consent to participate

Not applicable

Consent for publication

Not applicable

* The Declarations section must be placed before the Reference section.
a. Funding (information that explains whether and by whom the research was supported)
b. Conflicts of interest/Competing interests (include appropriate disclosures)
c. Availability of data and material (data transparency)
d. Code availability (software application or custom code)
e. Ethics approval (include appropriate approvals or waivers)
f. Consent to participate (include appropriate statements)
g. Consent for publication (include appropriate statements)
h. Authors' contributions (optional: please review the submission guidelines from the journal whether statements are mandatory)
>If any of the sections are not relevant to your manuscript, please include the heading and write 'Not applicable' for that section.

References

[1] N. H. Ononiwu, E. T. Akinlabi, C. G. Ozoegwu, and V. S. Aigbodion (2020) A Concise review of the effects of hybrid particulate reinforced aluminium metal matrix composites on the microstructure, density and mechanical properties in Lecuture Notes in Mechanical Engineering: Advances in Manufacturing Engineering, S. E. Seyed, A. Mokhotar, and F. Yusof, Eds. Springer Singapore: 433–443. https://doi.org/10.1007/978-981-15-5753-8_40

[2] O. M. Ikumapayi, E. T. Akinlabi, O. O. Abegunde, and O. S. I. Fayomi (2020) Electrochemical investigation of calcined agrowastes powders on friction stir processing of aluminium-based matrix composites. Materials Today: Proceedings. doi: 10.1016/j.matpr.2020.02.906

[3] R. G. Rao, M. Ghosh, R. I. Ganguly, S. C. Bose P, and K. L. Sahoo (2020) Mechanical properties and age hardening response of Al6061 alloy based composites reinforced with fly ash. Materials

Science and Engineering A. 772(138823): 1-8. doi: 10.1016/j.msea.2019.138823
[4] V. B. Kurapati and R. Kommineni (2017) Effect of wear parameters on dry sliding behavior of Fly Ash/SiC particles reinforced AA 2024 hybrid composites. Materials Research Express 4(096512): 1-8. doi: 10.1088/2053-1591/aa8a3e
[5] Aalco - Ferrous and Non-Ferrous Metals Stockist (2020). Aluminium Alloys - Aluminium 6082 Properties, Fabrication and Applications. AZoM. https://www.azom.com
[6] M. S. Prabhu, A. E. Perumal, S. Arulvel, and R. F. Issac (2019) Friction and wear measurements of friction stir processed aluminium alloy 6082 / $CaCO_3$ composite. Measurement 142: 10–20. doi: 10.1016/j.measurement.2019.04.061
[7] W. Jiang, J. Zhu, G. Li, F. Guan, Y. Yu, and Z. Fan (2021) Enhanced mechanical properties of 6082 aluminum alloy via SiC addition combined with squeeze casting. Journal of Materials Science andTechnology 88: 119–131. doi: 10.1016/j.jmst.2021.01.077
[8] K. Ravi Kumar, T. Pridhar, and V. S. Sree Balaji (2018) Mechanical properties and characterization of zirconium oxide (ZrO_2) and coconut shell ash(CSA) reinforced aluminium (Al 6082) matrix hybrid composite. Journal of Alloys and Compounds 765: 171–179. doi: 10.1016/j.jallcom.2018.06.177
[9] N. Henry, E. T. Akinlabi, and C. G. Ozoegwu (2020) Optimization techniques applied to machinability studies for turning aluminium metal matrix composites : A literature review. Materials Today: Proceedings. doi: 10.1016/j.matpr.2020.11.228
[10] P. A. Sylajakumari and R. Ramakrishnasamy (2018) Taguchi Grey Relational Analysis for Multi-Response optimization of wear in co-continuous composite. Materials 11(1743): 1-17. doi: 10.3390/ma11091743
[11] Z. Hussain, S. Khan, and P. Sarmah (2020) Optimization of powder metallurgy processing parameters of Al_2O_3 /Cu composite through Taguchi method with Grey relational analysis. Journal of King Saud University - Engineering Sciences 32(4): 274–286, 2020. doi: 10.1016/j.jksues.2019.01.003
[12] S. A. A. Daniel, R. Pugazhenthi, R. Kumar, and S. Vijayananth (2019) Multi objective prediction and optimization of control parameters in the milling of aluminium hybrid metal matrix composites using ANN and Taguchi -grey relational analysis. Defence Technology 15(4): 545–556. doi: 10.1016/j.dt.2019.01.001
[13] T. Thankachan et al. (2019) Prediction of surface roughness and material removal rate in wire electrical discharge machining on aluminum based alloys/composites using Taguchi coupled Grey Relational Analysis and Artificial Neural Networks. Applied Surface Science 472(2019): vol. 472. doi: 10.1016/j.apsusc.2018.06.117
[14] J. P. Ajithkumar and M. Anthony Xavior (2019) Cutting force and surface roughness analysis during turning of Al 7075 based hybrid composites. Procedia Manufacturing 30: 180–187. doi: 10.1016/j.promfg.2019.02.026
[15] J. Udaya Prakash, S. Ananth, G. Sivakumar, and T. V. Moorthy (2018) Multi-Objective Optimization of Wear Parameters for Aluminium Matrix Composites (413/B_4C) using Grey Relational Analysis. Materials Today: Proceedings. 5(2): 7207–7216. doi: 10.1016/j.matpr.2017.11.387
[16] M. M. Barzani, S. Farahany, and V. Songmene (2017) Machinability characteristics, thermal and mechanical properties of Al-Mg_2Si in-situ composite with bismuth. Measurement: Journal of the International Measurement Confederation, vol. 110, pp. 263–274, 2017, doi: 10.1016/j.measurement.2017.06.028
[17] R. Jiang, X. Chen, R. Ge, W. Wang, And G. Song (2018) Influence of TiB_2 particles on machinability and machining parameter optimization of TiB_2/Al MMCs. Chinese Journal of Aeronautics 31(1): 187–196, 2018. doi: 10.1016/j.cja.2017.03.012

[18] A. Pugazhenthi, I. Dinaharan, G. Kanagaraj, and J. D. R. Selvam (2018) Predicting the effect of machining parameters on turning characteristics of AA7075/TiB_2 in situ aluminum matrix composites using empirical relationships. Journal of the Brazilian Society of Mechanical Sciences and Engineering 40(555): 1-15. doi: 10.1007/s40430-018-1480-2

[19] K. S. Prakash, P. M. Gopal, and S. Karthik (2020) Multi-objective optimization using Taguchi based grey relational analysis in turning of Rock dust reinforced Aluminum MMC. Measurement 157(107664). doi: 10.1016/j.measurement.2020.107664

[20] D. Das, B. C. Routara, B. K. Nanda, and S. Chakraborty (2019) Machining Performance of Aluminium 7075 Composite: A Grey Based Taguchi Concept. International Journal of Innovative Technology and Exploring Engineering 9(2): 81–92. doi: 10.35940/ijitee.A4964.129219

[21] N. Henry Ononiwu, E. T. Akinlabi, and C. G. Ozoegwu (2019) Sustainability in Production and Selection of Reinforcement particles in Aluminium Alloy Metal Matrix Composites: A Review. Journal of Physics: Conference Series 1378(042015): 1-10. doi: 10.1088/1742-6596/1378/4/042015

[22] S. B. Hassan and V. S. Aigbodion (2013) Effects of eggshell on the microstructures and properties of Al–Cu–Mg/eggshell particulate composites. Journal of King Saud University - Engineering Sciences 27(1): 49–56. doi: 10.1016/j.jksues.2013.03.001

[23] J. Joel and M. Anthony Xavior (2018) Aluminium Alloy Composites and its Machinability studies; A Review. Materials Today: Proceedings 5(5): 13556–13562. doi: 10.1016/j.matpr.2018.02.351

[24] C. J. Nicholls, B. Boswell, I. J. Davies, and M. N. Islam (2017) Review of machining metal matrix composites. International Journal of Advanced Manufacturing Technology. 90(9–12): 2429–2441. doi: 10.1007/s00170-016-9558-4

[25] F. Puh, Z. Jurkivic, M. Perinic, M. Brezocnik, and S. Bulijan (2016) Optimization of Machining parameters for turning operation with multiple quality characteristics using Grey Relational Analysis. Technicki Vjesnik 23(2): 377–382. doi: 10.17559/TV-20150526131717

[26] S. Bose, A. Pandey, and A. Mondal (2018) Comparative analysis on aluminum-silicon carbide hybrid green metal matrix composite materials using waste egg shells and snail shell ash as reinforcements. Materials Today: Proceedings. 5(14): 27757–27766, 2018, doi: 10.1016/j.matpr.2018.10.011

[27] S. P. Dwivedi, A. K. Srivastava, N. K. Maurya, and M. Maurya (2019) Microstructure and mechanical properties of Al 6061/Al_2O_3/Fly-Ash composite fabricated through stir casting. Annales de Chimie: Science des Materiaux 43(5): 341–348. doi: 10.18280/acsm.430510

[28] S. Sharma and S. P. Dwivedi (2017) Effects of waste eggshells and SiC addition on specific strength and thermal expansion of hybrid green metal matrix composite. Journal of Hazardous Materials 333: 1–9. doi: 10.1016/j.jhazmat.2017.01.002

[29] Udaya and P. Fernandes (2019) Effect of fly ash and ball milling time on CNT-FA reinforced aluminium matrix hybrid composites. Materials Research Express 6(085027): 1-9. doi: 10.1088/2053-1591/ab1e20

[30] S. O. Akinwamide, S. M. Lemika, B. A. Obadele, O. J. Akinribide, B. T. Abe, and P. A. Olubambi (2019) Characterization and mechanical response of novel Al- (Mg – TiFe – SiC) metal matrix composites developed by stir casting technique. Journal of composite materials 53(28-30): 3929-3938. doi: 10.1177/0021998319851198

[31] I. Dinaharan, R. Nelson, S. J. Vijay, and E. T. Akinlabi (2016) Microstructure and wear characterization of aluminum matrix composites reinforced with industrial waste fly ash particulates synthesized by friction stir processing. Materials Characterization 118: 149–158. doi: 10.1016/j.matchar.2016.05.017

[32] C. R. Prakash Rao, M. S. Bhagyashekar, P. Chandra, and D. V. Ravikumar (2018) Effect of machining parameters on surface roughness while turning metal matrix composites-an

experimental approach. Materials Today: Proceedings 5(11): 24770–24779. doi: 10.1016/j.matpr.2018.10.275

[33] R. Kumar and S. Chauhan (2015) Study on surface roughness measurement for turning of Al 7075/10/SiCp and Al 7075 hybrid composites by using response surface methodology (RSM) and artificial neural networking (ANN). Measurement: Journal of the International Measurement Confederation 65: 166–180. doi: 10.1016/j.measurement.2015.01.003

[34] N. Sharma and K. Gupta (2019) Influence of coated and uncoated carbide tools on tool wear and surface quality during dry machining of stainless steel 304 Influence of coated and uncoated carbide tools on tool wear and surface quality during dry machining of stainless steel 304. Materials Research Express 6(086585): 1–19. doi: https://doi.org/10.1088/2053-1591/ab1e59

[35] D. Das, S. K. Pradhan, A. K. Sahoo, A. Panda, M. P. Satpathy, and C. Samal (2020) Tool wear and cutting force investigations during turning 15 wt% SiCp-Al 7075 metal matrix composite. Materials Today: Proceedings: 1–6. doi: 10.1016/j.matpr.2020.01.053

Figures

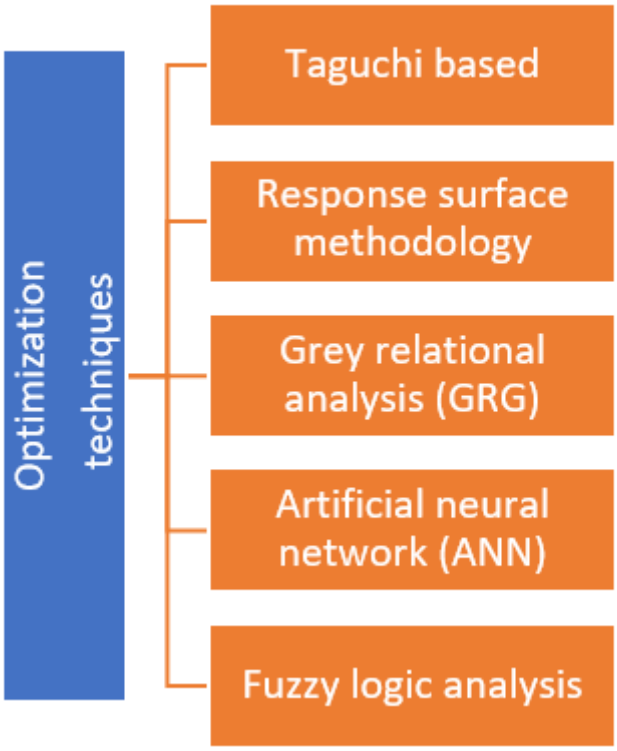

Figure 1

Optimization techniques applied for the machinability studies of AMCs

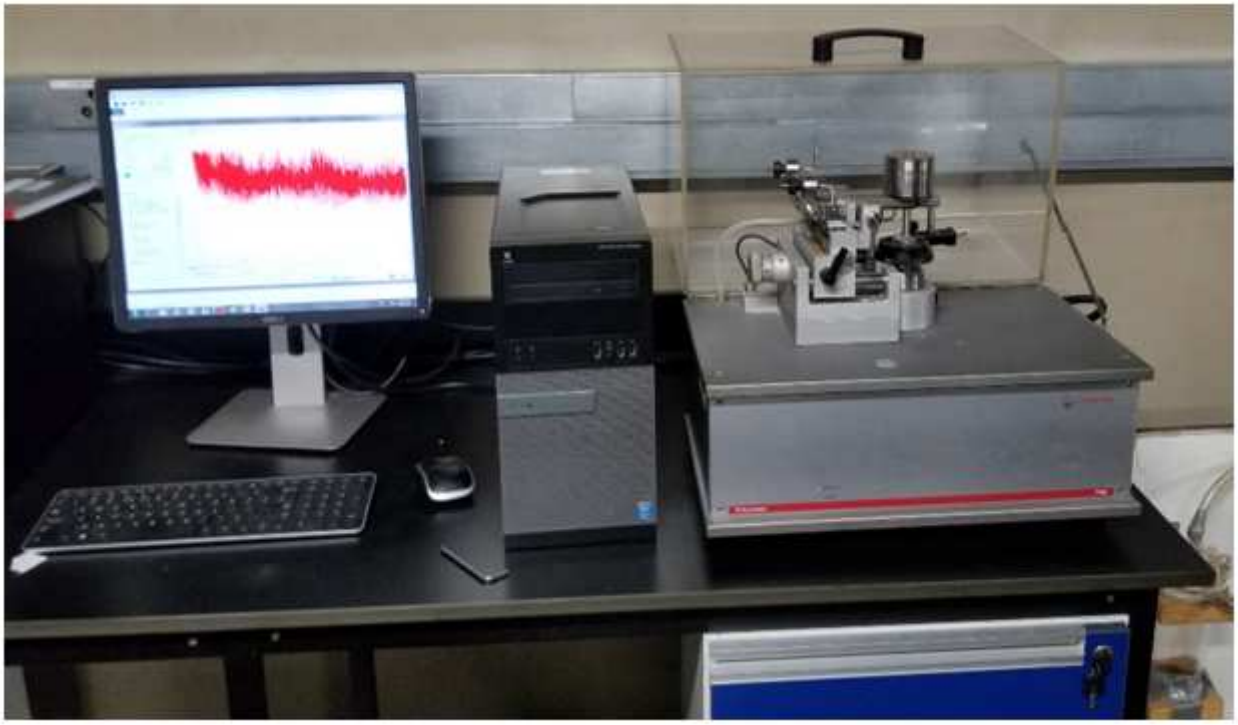

Figure 2

Antom Paar ball-on-disc tribometer

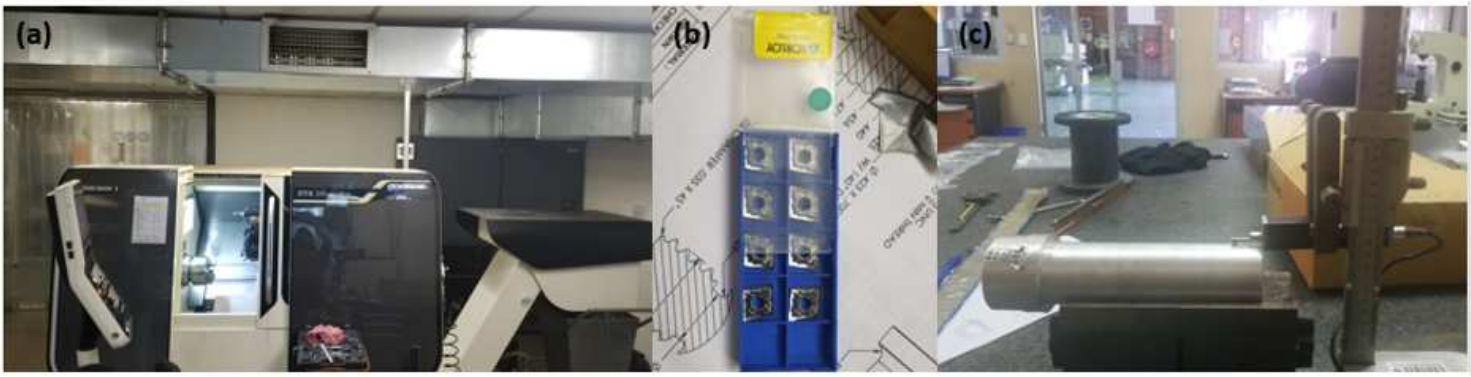

Figure 3

Equipment used to carry out the machinability analysis (a) CNC machine tool (b) Korloy single point cutting tool insert (c) Surface roughness tester

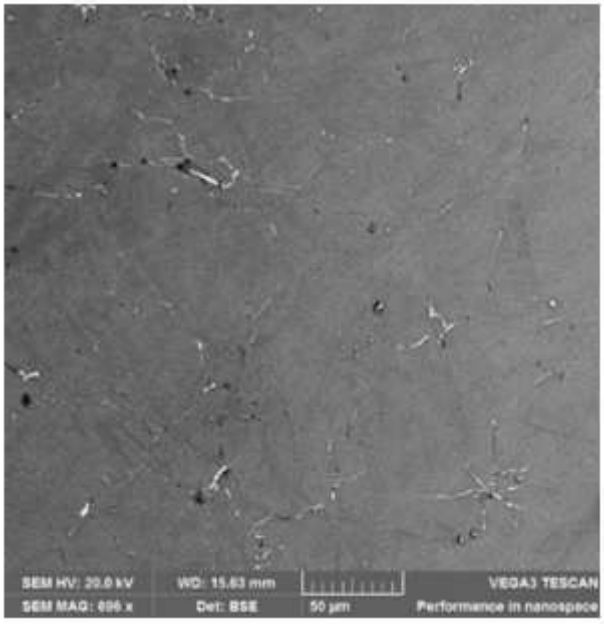

Figure 4

SEM micrographs of AA 6082/FA/CES

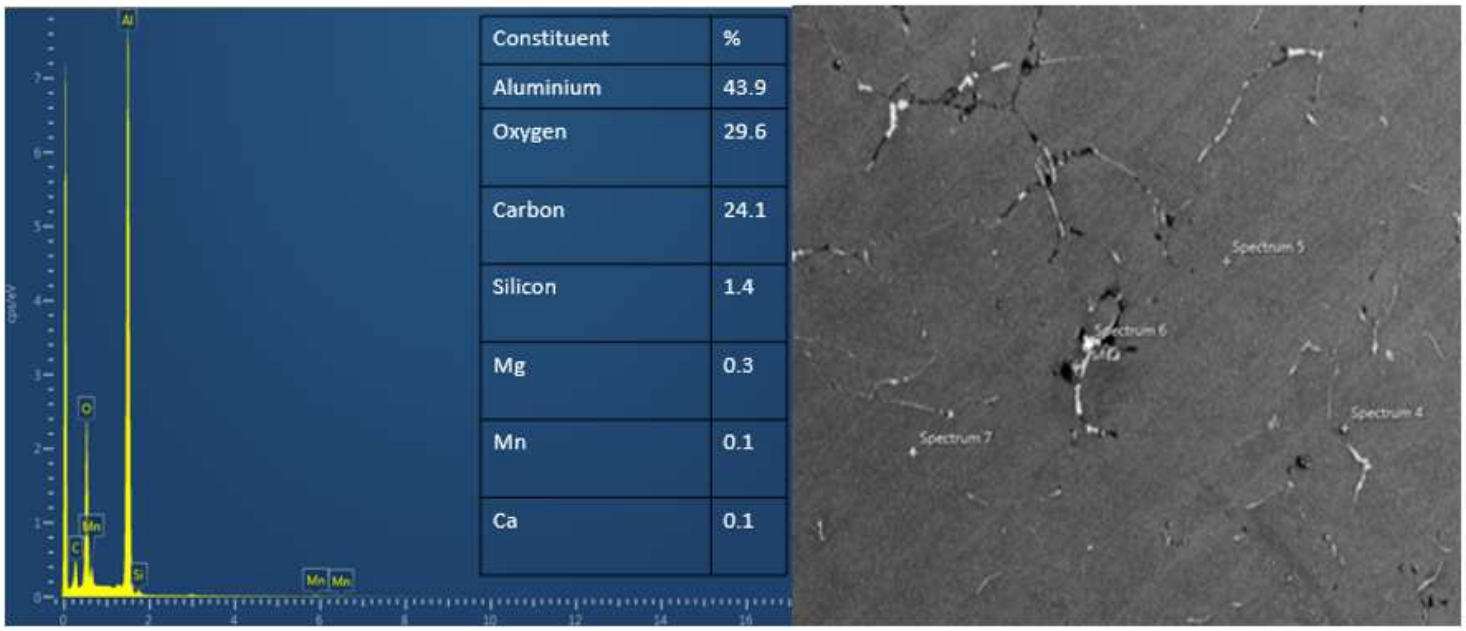

Figure 5

EDS analysis of AA6082/FA/CES

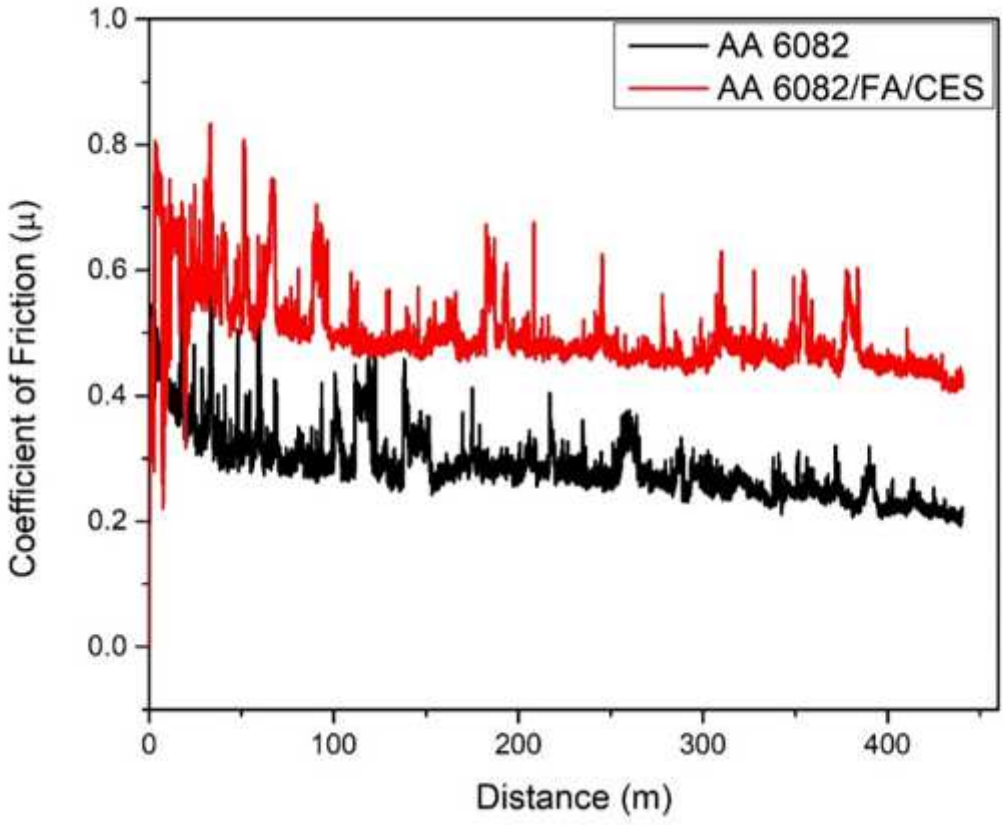

Figure 6

Coefficient of friction for the matrix and hybrid AMC

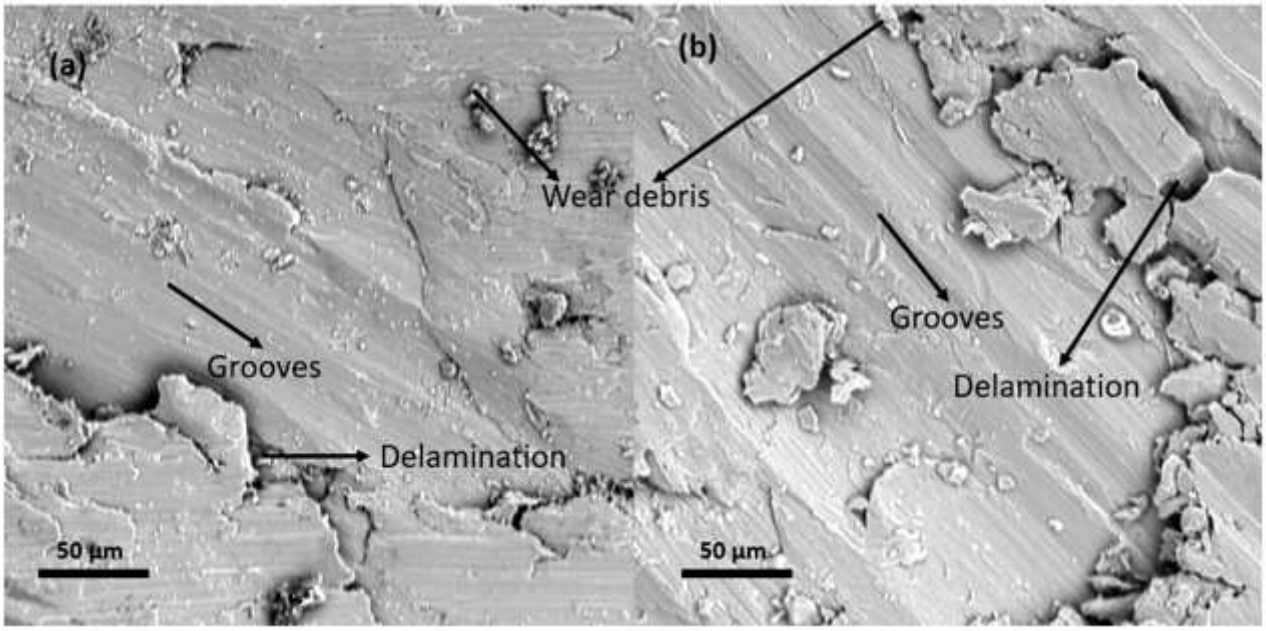

Figure 7

Micrographs of the wear mechanism for (a) AA 6082 (b) AA 6082/FA/CES

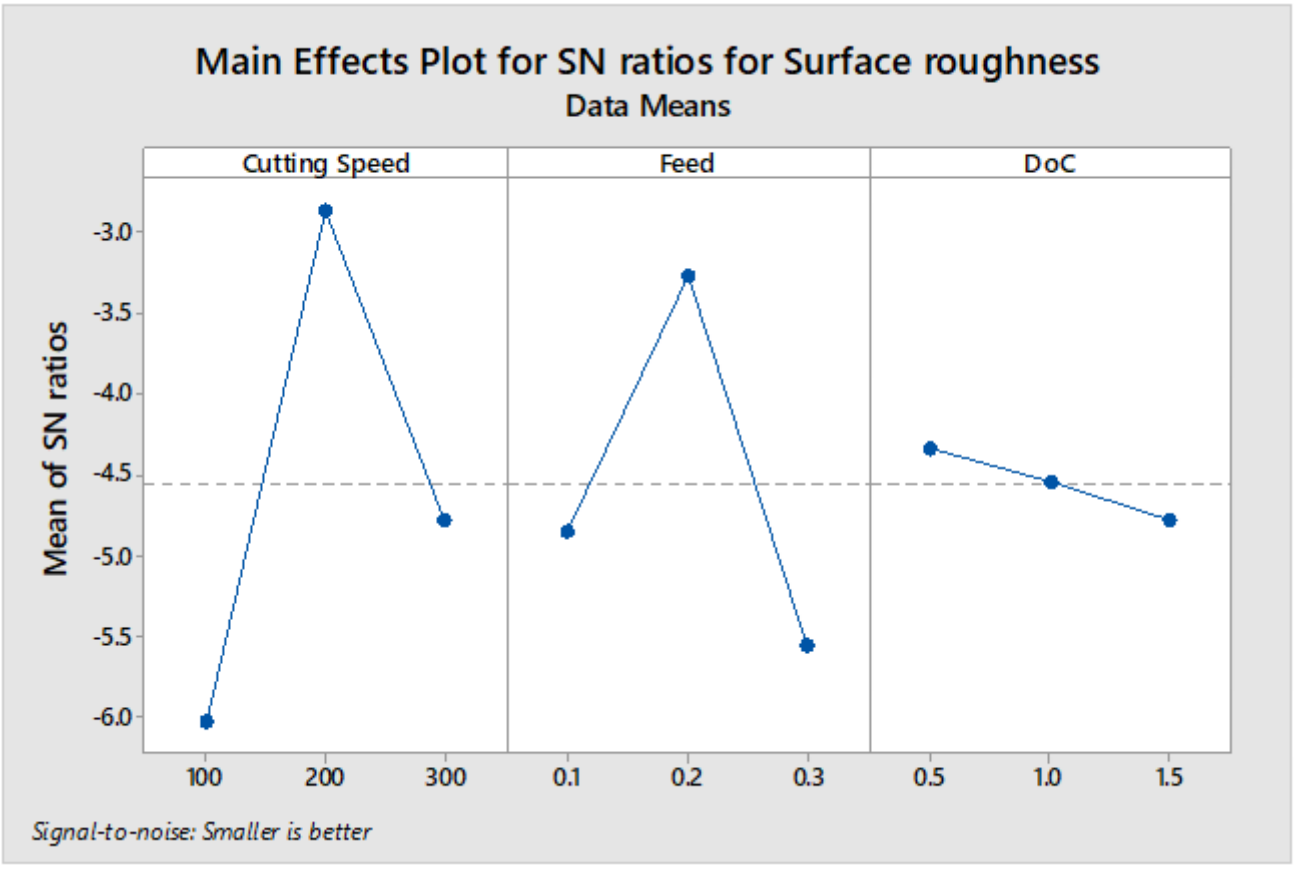

Figure 8

Main effects plots for S/N ratio of surface roughness

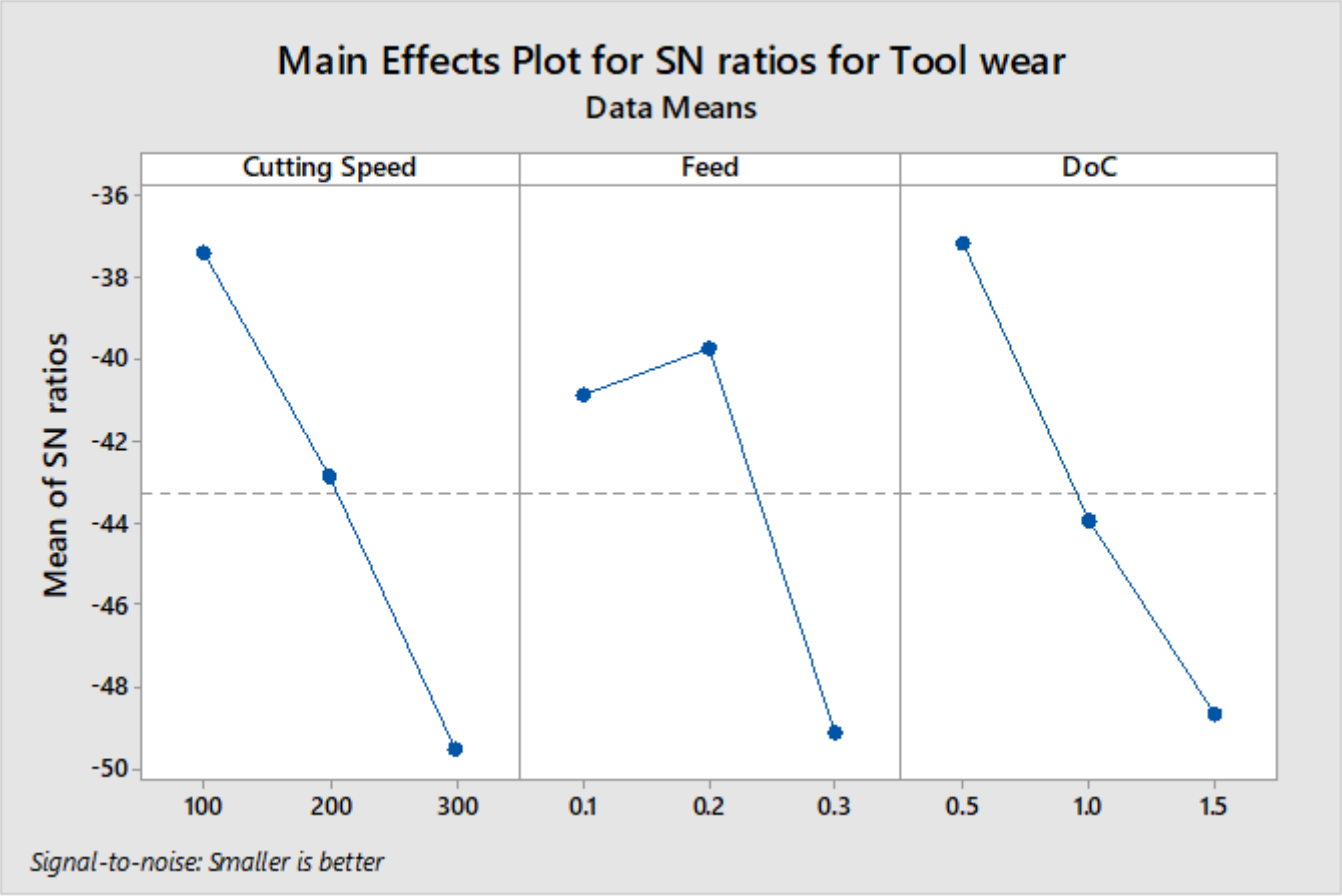

Figure 9

Main effects plots for S/N ratio of tool wear

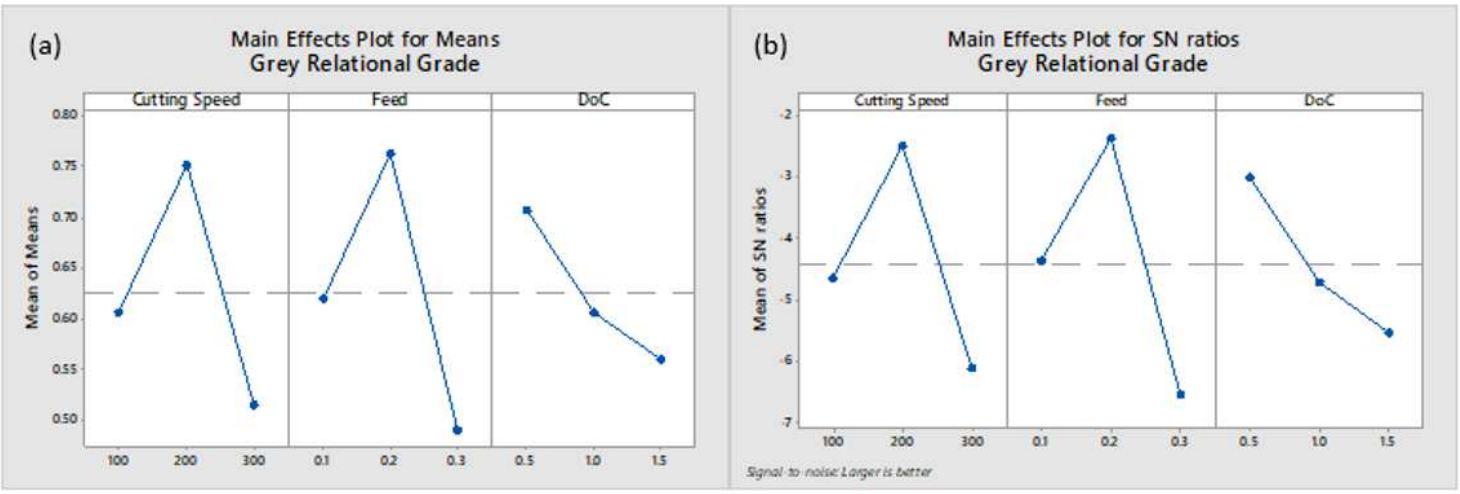

Figure 10

(a) Main effects plot for means of GRG (b) Main effects plots for S/N ratio of GRG

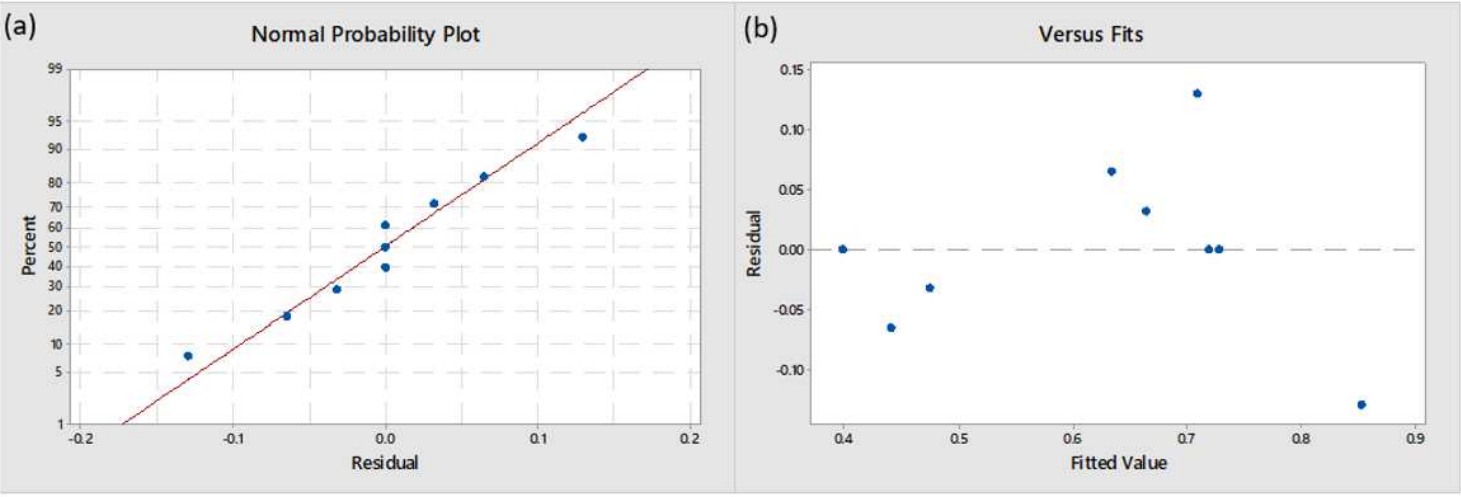

Figure 11

(a) Normal probability plots (b) Residual vs fits plot for the developed 2nd order regression model

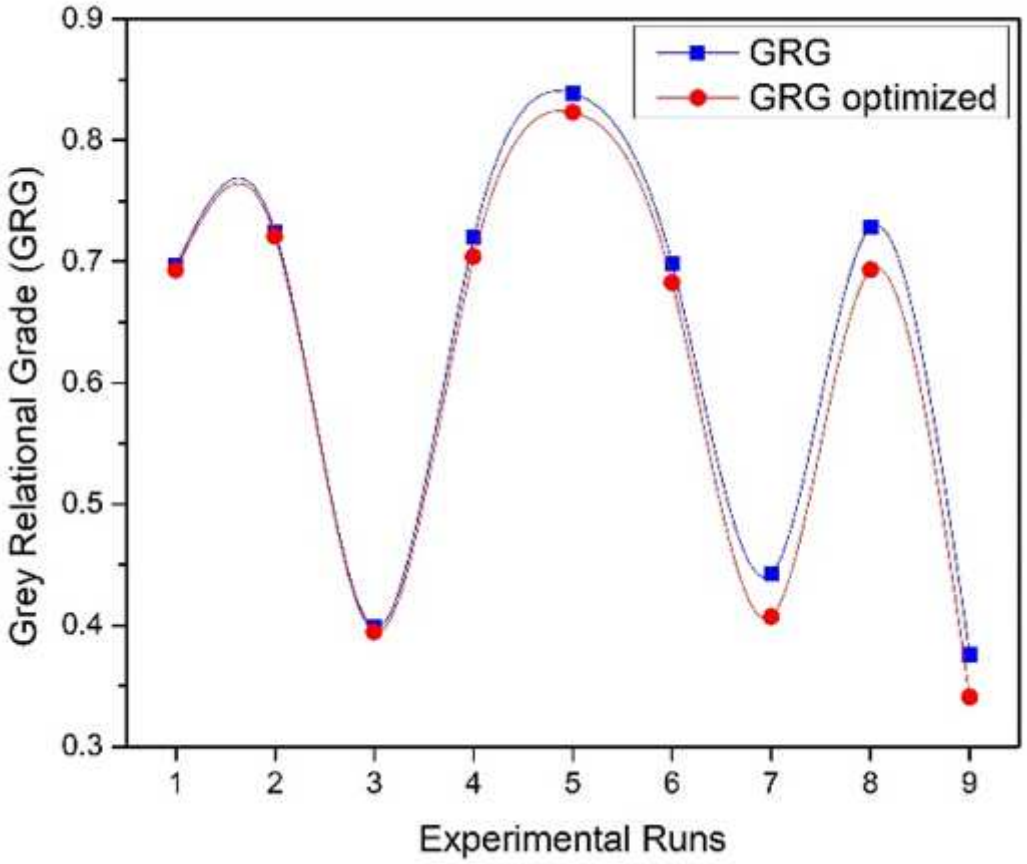

Figure 12

Comparison between the actual and predicted GRG for the experimental runs

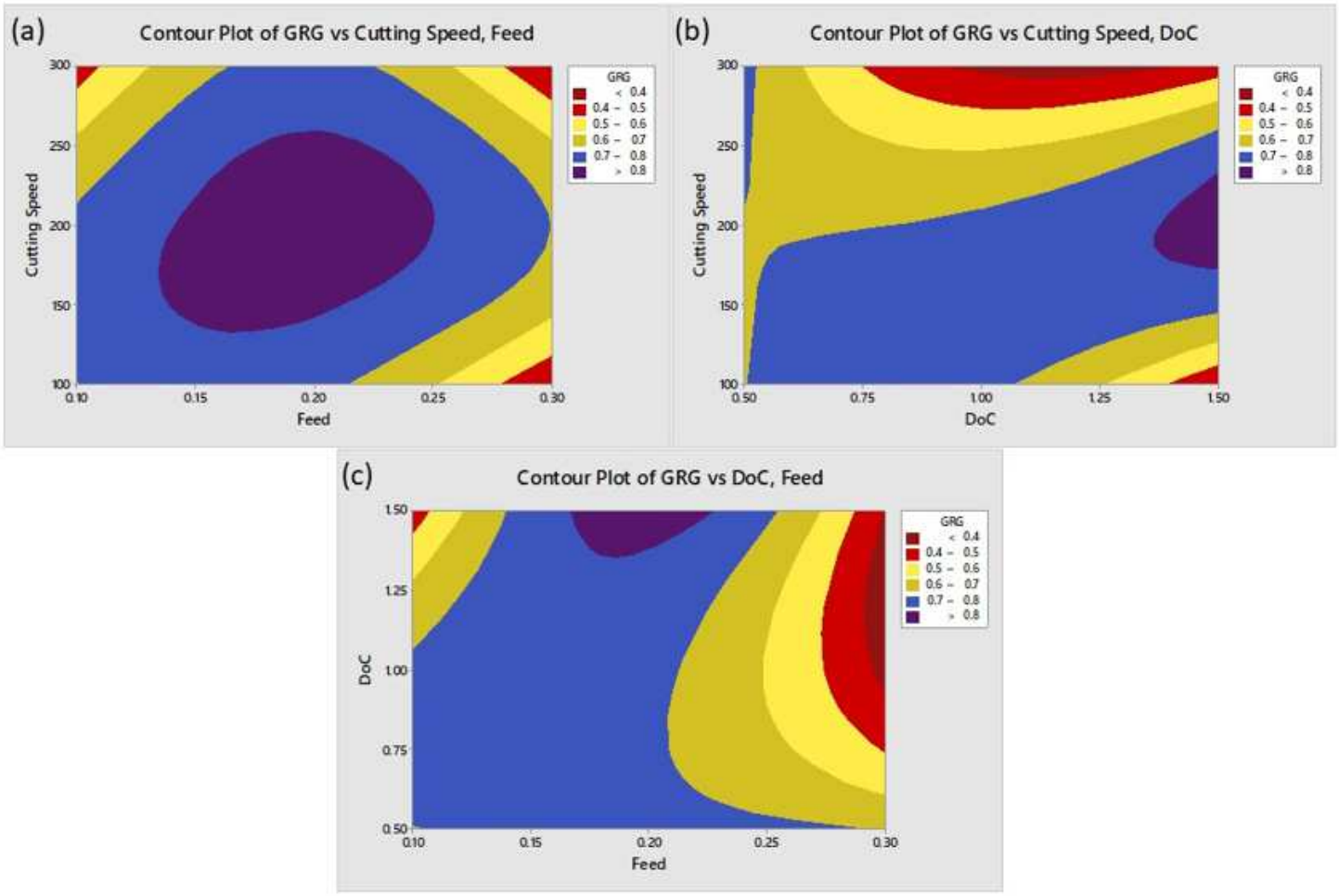

Figure 13

Contour plots for Grey relation grade against (a) Cutting speed and feed (b) cutting speed and depth of cut (c) depth of cut and feed